On Plasma Rotation with Toroidal Magnetic Field Ripple and no External Momentum Input

C. Fenzi, X. Garbet, E. Trier[1], P. Hennequin[1], C. Bourdelle, T. Aniel, G. Colledani, P. Devynck, C. Gil, Ö. Gürcan[1], L. Manenc, M. Schneider, J.-L. Segui and the Tore Supra team

CEA, IRFM, F-13108 St. Paul-lez-Durance, France.
[1]Ecole Polytechnique, LPP, CNRS, F-91128 Palaiseau cedex, France

E-mail contact of main author: christel.fenzi@cea.fr

Abstract. Ripple induced thermal loss effect on plasma rotation is investigated in a set of Ohmic L-mode plasmas performed in Tore Supra, and comparisons with neoclassical predictions including ripple are performed. Adjusting the size of the plasma, the ripple amplitude has been varied from 0.5% to 5.5% at the plasma boundary, keeping the edge safety factor constant. The toroidal flow dynamics is understood as being likely dominated by turbulence transport driven processes at low ripple amplitude, while the ripple induced toroidal friction becomes dominant at high ripple. In the latter case, the velocity tends remarkably towards the neoclassical prediction (counter-current rotation). The radial electric field is not affected by the ripple variation and remains well described by its neoclassical prediction. Finally, the poloidal velocity is fairly close to the neoclassical prediction at high ripple amplitude, but significantly departs from it at low ripple.

I. INTRODUCTION

In tokamak fusion plasmas, the rotation velocity plays a crucial role for the plasma performance. In particular, it is widely believed that a strong shear in the component of the rotation associated with the radial electric field is a key factor for turbulent transport reduction, both in advanced operation scenarios and edge transport barrier regimes [1-3]. Also, strong plasma rotation has a beneficial effect on MHD stability, by preventing mode locking and the onset of resistive wall mode [4] and neoclassical tearing modes [5]. In present day devices, strong plasma rotation is mainly driven by Neutral Beam Injection (NBI) heating which provides a significant external momentum source. Nevertheless in a fusion reactor or ITER, NBI is not expected to provide much external momentum. The plasma heating will be mainly provided by alpha particles, which imparts a small net torque on the plasma only [6], so that plasma rotation is expected to be lower compared to present devices. Consequently, understanding plasma rotation in low external momentum input condition is of major interest.

Plasma rotation is thought to result from a competition between turbulent transport processes [7-9] MHD effects [10-12], fast particle effects [13-17] and the ripple-induced toroidal friction [18-20]. The Toroidal magnetic Field (TF) ripple issue and its effect on plasma rotation are risen again nowadays after intensive studies regarding neoclassical aspects in the early nineties [21-25], recently reviewed in [26]. Because the TF ripple can not be entirely eliminated in any tokamak ($\delta <$ 0.5-1.2 % in ITER at the plasma boundary depending on insert configuration, with $\delta = (B_{\max} - B_{\min})/(B_{\max} + B_{\min})$ being defined as the relative amplitude of the toroidal magnetic field variation, where $B_{\max}$ is the TF under a TF coil and $B_{\min}$ is the TF between two coils), there always exists ripple induced non ambipolar particle fluxes. Whether or not the ripple induced toroidal friction could have a non negligible effect on plasma rotation, and how this effect competes with turbulence driven rotation for example, are important issues in view of ITER low torque scenarios. So far, the questions of the TF ripple effect on plasma rotation and comparison with *standard* neoclassical predictions, i.e. non-accounting for the neoclassical ripple-induced toroidal friction, have been mostly addressed in JET [27-30] and JT-60U [31-33], but in a limited range of ripple amplitudes.

Tore Supra is a large size tokamak with no external momentum input and a relatively strong TF ripple (up to 7% at the plasma boundary in standard plasma conditions, in contrast to the ~ 0.08% standard value in JET for example), which makes the device particularly well suited for studying ripple effect on plasma rotation since associated neoclassical effects are expected not to be negligible. In this paper, we focus on ripple-induced thermal particle loss effect and report experimental observations of plasma rotation in L-mode ohmic plasmas, with no external momentum input and TF ripple amplitude ranging from 0.5% to 5.5% at the plasma boundary. Neoclassical predictions including ripple [26] are summarized in Section II and compared with radial electric field, toroidal and poloidal velocity profiles in Section III. We find that the toroidal velocity increments in the counter-current direction when the ripple amplitude increases, and converges towards the neoclassical prediction at high ripple value. The toroidal flow dynamics is therefore understood as being dominated by turbulence transport processes at low ripple value, then transiting towards a transport regime dominated by the neoclassical ripple-induced toroidal friction at high ripple. The radial electric field is not affected when the ripple amplitude increases and remains well described by neoclassical predictions. The dynamics of the poloidal flow appears somehow more complex and is not understood yet. The poloidal velocity is found not to be far from neoclassical predictions at high ripple amplitude, but departs significantly from it at low ripple. Those observations are discussed in Section IV.

II. NEOCLASSICAL PREDICTIONS INCLUDING THERMAL RIPPLE EFFECT

Neoclassical predictions accounting for the ripple induced thermal toroidal friction (i.e. related to thermal ripple losses only, and not fast particles) have been recently revisited and clarified in [26], in the limit of large aspect ratio. It appears that several transport regimes and sub-regimes can coexist on a same magnetic flux surface depending on the ripple amplitude and the plasma collisionality as summarized in tables I and II where ε is the inverse aspect ratio, δ is the ripple amplitude at plasma boundary, q is the safety factor, N in the number of toroidal coils (18 in Tore Supra) and ν^* is the plasma collisionality. In the general case, it is expected that in order to compensate the ripple induced radial fluxes of ions trapped in local ripple wells, the radial electric field E_r evolves and adjusts itself to ensure ambipolarity. In a single light species plasma ($Z_i = 1$, deuterium), this implies that E_r can be approximated by $E_r = T_i(\nabla n_i/n_i + k_E \nabla T_i/T_i)/eZ_i$ where n_i is the ion density, T_i is the ion temperature and k_E = [1.5 − 3.37] depending on the ripple amplitude and the plasma collisionality (provided $E\times B$ drift effects, which are expected to lower non ambipolar fluxes [21], are ignored). The poloidal velocity appears not to be strongly affected by ripple effect and reads as the neoclassical standard expression, $V_\theta = k_P \nabla T_i / eZ_i B$ where k_P = [-0.5 − 1.17]. Hence the toroidal velocity (inferred from the radial force balance equation) reads as $V_\phi = k_T \nabla T_i / eZ_i B_\theta$ where k_T = [1.67 − 3.54], i.e. it is predicted counter-current always. However in the limit of local trapping regime with ν* >1 (table I), the toroidal velocity is predicted to be zero which is unrealistic.

regime	local trapping	
coll.	$\nu^* < \left(\frac{\delta}{\varepsilon}\right)^{3/2}$	$\nu^* >> 1$
k_E	3.37	**1.5**
k_P	1.17	**-0.5**
k_T	3.54	**0**

TABLE I: Neoclassical local trapping regimes depending on the plasma collisionality (see [26] for more detail; values of interest are reported in bold here).

regime	no local trapping and $\frac{\delta}{\varepsilon} >> \frac{1}{(Nq)^{3/2}}$		
	banana-drift weakly collisional	ripple-plateau weakly collisional	ripple-plateau collisional
coll.	$\nu^* << \frac{1}{N^2 q^2}$	$\frac{1}{N^2 q^2} << \nu^* << Nq\left(\frac{\delta}{\varepsilon}\right)^2$	$Nq\left(\frac{\delta}{\varepsilon}\right)^2 << \nu^*$
k_E	3.37	1.5	**1.5**
k_P	1.17	1.17	**1.17**
k_T	3.54	1.67	**1.67**

TABLE II: Neoclassical regimes and sub-regimes without local trapping, and various collisionality limits (see [26] for more details; values of interest are reported in bold here).

In previous works [34,35], it has been checked that radial electric field measurements in Tore Supra agrees well with the ripple-induced E_r prediction in the outer part of the plasma and in various heating regimes, suggesting that the main contribution in the ambipolarity condition determining E_r comes from ripple induced thermal particle fluxes as also mentioned in [36]. This raises the issue of the toroidal and poloidal velocity behaviours, and to which extend they are described by neoclassical predictions.

III. MEASUREMENT TECHNIQUES

Rotation profiles are measured in Tore Supra with the Charge eXchange Recombination Spectroscopy (CXRS) system, which has been significantly enhanced in order to improve its spatial coverage, time resolution and measurement accuracy [37,38]. The system uses a diagnostic NBI and provides measurements of T_i and V_Φ profiles, as well as n_i profiles from CVI line analysis, assuming that the carbon impurity has the same velocity and temperature as the main ions. Fifteen tangential viewing lines are used, with 2 cm spatial resolution at the plasma edge and 6 cm in the core. For the plasmas to be discussed here, the spatial coverage extends from the plasma centre to r/a ~ 0.95 in the equatorial plane (where r/a is the normalized minor radius), and the time resolution is 100ms. Short and low power beam pulses are used for the measurements (hydrogen beam, 300ms pulse, injected energy E_{inj} = 55keV, power P = 350kW, perpendicular injection), so that the momentum carried out by injected particles can be neglected. Radial electric field measurements are performed using Doppler reflectometry (DR) technique [39]. The system provides local measurements of the density fluctuation perpendicular velocity in the laboratory frame, that is $u_\perp = V_{E\times B} + V_{fluc} \cong -E_r / B$ where $V_{E\times B} = E\times B / B^2$ and V_{fluc} is the mean fluctuation phase velocity. The latter contribution to $u_\perp$ is small indeed, of the order of the diamagnetic drift velocity (provided there is no major change in the turbulence regime nor in its phase velocity). Consequently, $u_\perp$ is most often dominated by the E×B term contribution as observed on several tokamaks and stellerators in various plasma conditions [40-44], and supported by linear gyrokinetic calculations as performed in Tore Supra [39] with KINEZERO [45]. Hence the poloidal velocity profiles can be evaluated from the radial force balance equation, combining CXRS and DR measurements or E_r neoclassical prediction (most often, CXRS and DR measurement locations do not entirely overlap), since the latter can be used confidently as mentioned in Section II.

IV. EXPERIMENTAL RESULTS

The plasmas to be discussed here were performed in Ohmic L-mode at B_T = 2.1T. In order to vary the ripple amplitude, the size of the plasma was varied with a minor radius ranging from

55cm to 72cm, while the plasma current was adjusted between 0.5MA and 0.85MA with central density n_{e0} = 4 – 4.5×10^{19}m^{-3} in order to keep the edge safety factor q_a~3.3 constant and similar plasma edge properties. In consequence, the TF ripple magnitude could be varied

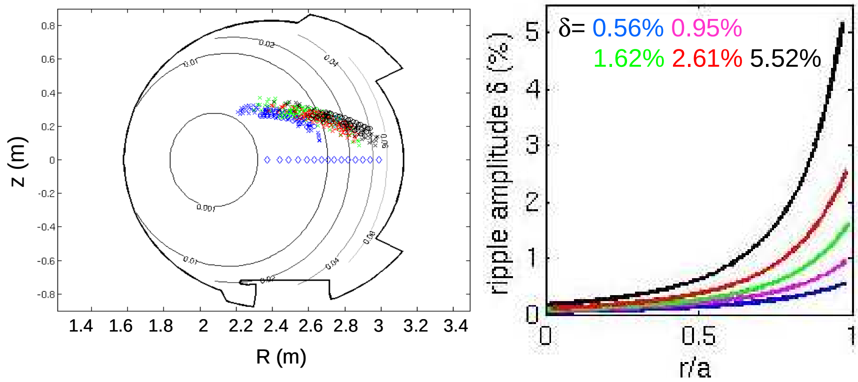

Figure 1: Iso-ripple curves in Tore Supra, with CXRS (diamonds) and DR (circles and crosses) measurement locations for the set of analyzed discharges. Right: associated ripple amplitudes.

from ~ 0.5% to 5.5% at the plasma boundary (Figure 1). The electron temperature was kept rather low (T_{e0} = 0.75 – 1.2keV), and no significant changes were observed on T_i profiles (T_{i0} ~ 750eV). Provided the plasma collisionality and ripple amplitudes, the ripple-plateau collisional sub-regime condition described in table II (with $\delta/\varepsilon >> 1/N^2q^2$) is found to apply in most plasma cases, over the plasma region 0.6 > r/a > 0.1 (where ν^* < 1). For r/a < 0.1 and r/a > 0.6 (ν^* > 1), as in the lower ripple plasma cases (for which ν^* > 1 over the full plasma radius), local trapping regime condition applies as reported in table I.

Toroidal Velocity The toroidal rotation velocity evolution with the ripple amplitude is illustrated in Figure 2. The whole plasma appears to rotate in the co-current direction (positive velocity) at low ripple amplitude (δ = 0.56%). When the ripple amplitude increases, the toroidal rotation velocity becomes counter-current in the edge (for r/a > 0.6) while it remains co-current though flattening in the core (see δ = 1.62% for instance), then shifts to pure hollow counter-current rotation at the highest ripple amplitude (δ = 5.52%). This behaviour is consistent with JET [30] and JT-60U [32] observations, and similar to static nonresonant error field perturbation effect on toroidal rotation reported in DIII-D [46].

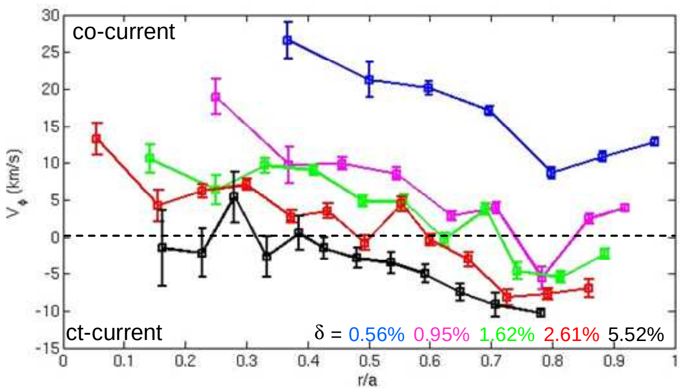

Figure 2: V_Φ profile evolution with the ripple amplitude. Positive resp. negative velocities refer to co-current resp. ct-current direction.

Comparisons with neoclassical ripple-plateau regime predictions (k_T = 1.67) are detailed in Figure 3 for ripple amplitudes δ = 0.56%, 1.62%, 5.52%. When the ripple amplitude increases, the toroidal velocity clearly evolves towards the neoclassical prediction with a good agreement in term of magnitude and direction in the highest ripple case. As mentioned above, local trapping regime predictions (k_T = 0) apply for r/a > 0.6, r/a < 0.1, as for the δ = 0.56%

plasma case. Therefore, the full radius comparison with the ripple-plateau regime prediction is given for completion.

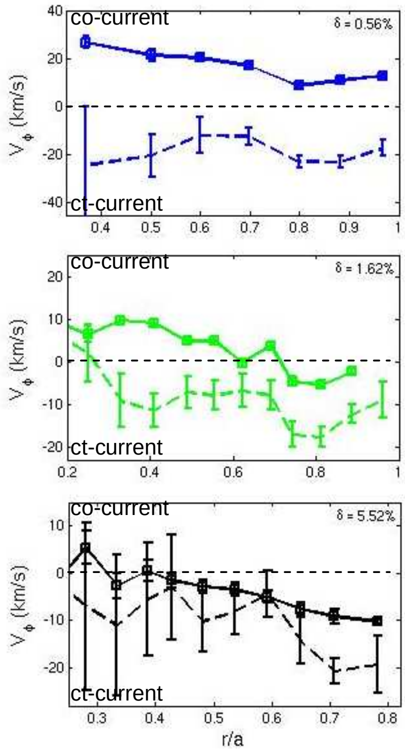

Figure 3: Comparison between measurements (solid curves, squares) and ripple-plateau neoclassical predictions (dashed curves). Local trapping regime predictions ($\nu^* > 1$, $k_T = 0$) should apply for r/a > 0.6, r/a < 0.1, as for the $\delta = 0.56\%$ plasma case.

Radial electric field The radial electric field inferred from DR measurements (Figure 4) is not found to vary significantly with the ripple strength over the plasma

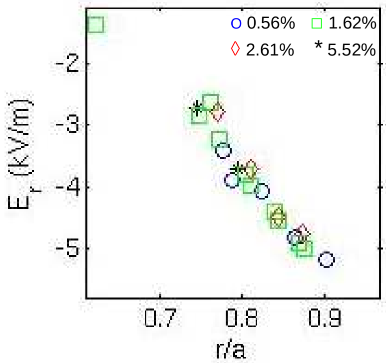

Figure 4: E_r profile measurements from DR for the δ = 0.56%, 1.62%, 2.61% and 5.52% plasma cases.

edge region mainly probed by the diagnostic in those discharges (*r/a* ~ 0.55 – 0.9).Also, it is found to agree well with ripple-plateau collisional regime predictions ($\nu^* > 1$, $k_E = 1.5$) as already reported in [34,35].

Poloidal velocity The above observations raise the question of the poloidal velocity behaviour with increasing ripple amplitude, since no T_i nor E_r but V_Φ modifications are significant. The plasma rotation velocity and the radial electric field E_r are linked through the radial ion force balance equation, $E_r = \nabla p_i / Z_i e n_i - V_{\theta,i} B_\phi + V_{\phi,i} B_\theta$ (valid for any plasma species *i*) where p_i is the ion pressure, Z_i the charge of the ion, *e* the electronic charge, n_i the ion density, B_θ and B_Φ are the poloidal and toroidal magnetic fields. V_θ profile evolution (main ions, deuterium D) with ripple is reported in Figure 5 in the same plasma cases as above, as inferred from the radial force balance equation, with V_Φ and T_i from CXRS measurements, E_r considered as neoclassical. Velocity profiles are found to be rather flat and positive (i.e. in the electron diamagnetic drift direction) at low ripple value. When the ripple increases, the velocity amplitude reduces and reverses sign at the edge. In the highest ripple case, the velocity is negative (ion diamagnetic drift direction). Since neoclassical predictions with ripple indicate that collisional viscous damping terms keep being dominant in the

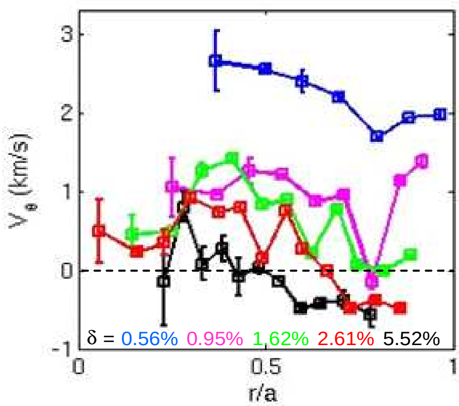

Figure 5: $V_{\theta,D}$ profile evolution with the ripple amplitude, as inferred from the radial force balance equation.

equilibrium poloidal flow dynamics (V_θ expressions are similar to those as standard neoclassical predictions depending on the plasma collisionality), measurements are compared with NCLASS [47] predictions in Figure 6. It clearly shows that the velocity tends to agree with the neoclassical prediction at high ripple, while it significantly departs from it at low ripple value.

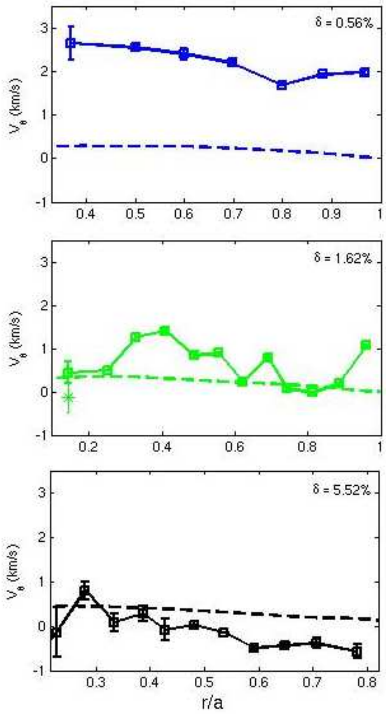

Figure 6: *Comparisons between $V_{\theta,D}$ inferred from the radial force balance equation (solid curves) and NCLASS predictions (dash curves).*

IV. DISCUSSION

A coherent picture can be clearly illustrated by the evolution of V_Φ with δ_{loc} (Figure 7), δ_{loc} being the local TF ripple at the CXRS measurement locations. As suggested in Section III, it shows that V_Φ is continuously decreasing with δ_{loc}, evolving from co-rotation to counter-rotation and approaching, for the largest δ_{loc}, the neoclassical prediction accounting for the ripple-induced thermal toroidal friction. Such behaviour strongly indicates a competition between two main driven rotation mechanisms. At low ripple value (δ = 0.56% case) V_Φ is co-current hence not neoclassical, and can be understood as dominated by turbulence driven contributions. When the ripple amplitude increases, the latter compete with ripple-induced thermal toroidal friction, which in term becomes strong enough to counter-balance turbulence driven terms and the velocity converges towards the counter-current neoclassical value (δ = 5.52% case). The scatter in V_Φ observed for δ_{loc} < 0.5% could then be explained by different local level of turbulence related to the experimental procedure.

The competition between turbulent momentum drive and neoclassical friction can be assessed by using the toroidal projection of the force balance equation, which is schematically of the form $dV_\phi / dt = F_{turb} + F_{neo}$. Here F_{turb} is minus the divergence of the turbulent Reynolds stress tensor Π, and F_{neo} is the collisional friction force due to ripple. The latter is of the form $F_{neo} = -\nu_{neo}\left(V_\phi - k_T V_{T\phi}^*\right)$ where k_T is a number, $V_{T\phi}^* = \nabla_r T_i / eB_\theta$ is the toroidal diamagnetic velocity, and ν_{neo} is the friction rate. In the ripple-plateau regime, an estimate of the friction rate (large aspect ratio) is $\nu_{neo} = \sqrt{\pi} G_2(\alpha) N \nu_{T_i} \delta^2 / 2R$ where v_{Ti} is the ion thermal velocity, R the major radius. The function G_2 is the ripple flux average, which is approximated by 1. In steady state, $F_{turb} + F_{neo} = 0$ and the toroidal rotation reads as $V_\phi = k_T V_{T\phi}^* - \nabla\Pi / \nu_{neo}$, with $\nu_{neo} \propto c / \sqrt{T_i}\,\delta^2$ where c in a constant. Consequently, the slope observed in the velocity trend

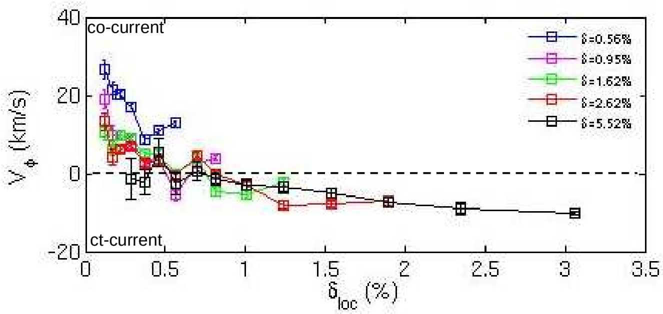

Figure 7: V_Φ at local ripple amplitude values δ_{loc} for the set of analyzed discharges.

in Figure 7 (varying as ~ $1/\delta^2$), could be interpreted as an indication on the turbulent Reynolds stress tensor magnitude, while the asymptotic value at high ripple is the neoclassical velocity. The Reynolds stress tensor is the cross-correlation between the radial and toroidal components of the velocity fluctuations, i.e. $\Pi = \langle \tilde{v}_r \tilde{v}_\phi \rangle$ where $\tilde{\boldsymbol{v}}$ is the turbulent velocity and the bracket is a statistical average over fluctuations. A quasi-linear calculation [48] yields the following expression $\Pi = -\chi_\phi \nabla_r V_\phi + v_\phi V_\phi + \Pi_{RS}$ where χ_ϕ is the turbulent viscosity, v_ϕ the velocity pinch velocity, and Π_{RS} is the residual stress. The latter is due to shear flow [8,49-51], up-down asymmetry [9], and gradient of turbulence intensity [52,53]. In these Ohmic discharges, shear flow is small, while the equilibrium is up-down symmetrical. Turbulence measurements usually show that the intensity gradient is large in the edge, but small in the core [54]. We therefore neglect the residual stress in the following. This approximation is certainly debatable, and would deserve further discussion on the basis of numerical simulations. This leaves the viscosity and the pinch velocity, likely due to curvature effects [55-57]. Unfortunately, the data available do not allow for a clear separation between those two quantities. We therefore introduce an effective viscosity $\chi_{\phi,eff}$ such that, $\Pi = -\chi_{\phi,eff}\, dV_\phi / dr$. The balance $F_{turb}+F_{neo}=0$ in steady-state yields an estimate of the effective velocity (regardless of sign consideration) $\chi_{\phi,eff} / L_V^2 \approx \nu_{neo} \Delta V_\phi / V_\phi$ where $\Delta V_\phi = \left| V_\phi - k_T V_{T\phi}^* \right|$ and L_V is a velocity gradient length (strictly speaking L_V^2 is related to the profile curvature). Putting numbers, one finds $\chi_{\phi,eff} \approx 2\sqrt{T_i}\left(10^3 \delta\right)^2 L_V^2 \Delta V_\phi / V_\phi$ (with T_i in keV). Applying this expression to Tore Supra data yield effective viscosity in the range of a few $m^2 s^{-1}$. This estimate is therefore in the right ballpark, though somewhat higher than expected for Ohmic plasmas.

The observed poloidal flow dynamics is not understood yet. In fact, the mismatch between the inferred poloidal velocity and neoclassical value can be attributed to two possible causes at least. One obvious cause is the turbulent generation of poloidal flow, in spite of a strong collisional viscous damping. Another possible source of discrepancy may come from the match between the fluctuation velocity $u_\perp$ measured by Doppler reflectometry and the $E \times B$ velocity $V_E=-E_r/B$. As mentioned before, the relationship between these two velocities is $u_\perp=-E_r/B+V_{fluc}$, where V_{fluc} is the mean fluctuation phase poloidal velocity in the co-moving plasma frame. Therefore, calling $V_{\theta,ref}$ the poloidal velocity deduced from the radial force balance equation ignoring V_{fluc} contribution to E_r, one finds that the true poloidal velocity reads $V_\theta = V_{\theta,ref} - V_{fluc}$. Since it is expected that V_θ matches the neoclassical value, i.e. close to zero since the collisionality regime is in between banana and plateau, one would need a fluctuation phase velocity that is positive, which would correspond to TEM. Although not impossible, the rather high values needed for V_{fluc} seem unlikely. Also this would contradict the good agreement between the radial electric field and the value predicted by the neoclassical theory. This is confirmed by linear gyrokinetic simulations with QuaLiKiz [58]: in those plasma discharges, the most unstable modes are ITG type modes and the fluctuation phase velocity (negative, ion magnetic drift direction) is found to be at r/a = 0.8 in the range of a few tens of ms^{-1}.

Acknowledgements The authors wish to thank L.-G. Eriksson for useful discussions and support. This work was carried out within the framework of the European Fusion Development Agreement and the French Federation for Fusion Studies. It is supported by the European Communities under the contract of Association between EURATOM and CEA, and the contract LRCV3232.001 between CEA and CNRS. The views and opinions expressed herein do not necessarily reflect those of the European Commission.

References

[1] K. H. Burrell, Science **281**, 1816 (1998)
[2] T. S. Hahm and K. H. Burrell, Phys. Plasmas **2,** 1648 (1995)
[3] E. J. Synakowski *et al*., Plasma Phys. Control. Fusion **40**, 581 (1993)
[4] A. M. Garofalo *et al.*, Nuc. Fusion **41**, 1171 2001
[5] R. Buttery *et al.*, Phys. Plasmas **15**, 056115 (2008)
[6] M. Schneider *et al*., Plasma Phys. Control. Fusion **47**, 2087 (2005)
[7] B. Coppi *et al.*, Nuc. Fusion **42**, 1 (2002)
[8] Ö. D. Gürcan *et al.*,Phys. Plasmas **14**, 042306 (2007)
[9] Y. Camenen *et al.*, Phys. Rev. Letters **102**, 125001 (2009)
[10] L.-G. Eriksson *et al.*, Plasma Phys. Control. Fusion **34**, 863 (1992)
[11] E. Lazzaro *et al.*, in Proceedings of 29th EPS Montreux 2002 EPS ECA Vol. 26B (2002)
[12] J.- M. Noterdaeme et al., Nuc. Fusion **43**, 274 (2003)
[13] W. Perkins *et al.*, Phys. Plasmas **8**, 2181 (2001)
[14] L.-G Eriksson *et al.*, Nuc. Fusion **41**, 91 (2001)
[15] L.- G. Eriksson *et al.*, Nuc. Fusion.**42**, 959 (2002)
[16] L.- G Eriksson *et al.*, Phys. Rev. Letters **92**, 135001 (2004)
[17] L.- G Eriksson *et al.*, Plasma Phys. Control. Fusion **51**, 044008 (2009)
[18] T. E. Stringer Nuc. Fusion, **12** 689 (1972)
[19] J. W. Connor and R. J. Hastie, Nucl. Fusion **13**, 221 (1973)
[20] P.N. Yushmanov, Review of Plasma Physics (Consultants Bureau, New York, 1990), Vol. 16
[21] P.N. Yushmanov, Nuc. Fusion **22**, 315 (1990)
[22] A.B. Mikhailovskii, Plasma Phys. Rep. **21**, 529 (1995)
[23] B. N. Kovrizhnykh *et al.*, Plasma Phys. Rep. **25**, 760 (1999)
[24] K. C. Shaing, Phys. Plasmas **10**, 1443 (2003)
[25] J.-K. Park *et al.*, Phys. Rev. Letters **102**, 065002 (2009)
[26] X. Garbet *et al.*, Phys. Plasmas **17**, 072505 (2010)
[27] K. Crombé *et al*., Phys. Rev. Letters **95**, 155003 (2005)
[28] P.C. DeVries *et al.*, Nuc. Fusion **48**, 035007 (2008)
[29] K. Crombé *et al*., Plasma Phys. Control. Fusion **51**, 055005 (2009)
[30] F. Nave *et al.*, Phys. Rev. Letters **105**, 105005 (2010)
[31] Y. Koide *et al*, Plasma Phys. Control. Nucl. Fusion Res. **1**, 777 (1993)
[32] M. Yoshida *et al.*, Plasma Phys. Control. Fusion **48**, 1673 (2006)
[33] H. Urano *et al.*, Nuc. Fusion **47**, 706 (2007)
[34] E. Trier *et al.*, Nuc. Fusion **48**, 092001 (2008)
[35] E. Trier PhD (2010)
[36] A. Romannikov *et al.*, Nuc. Fusion **40**, 319 (2000)
[37] C. Fenzi *et al.*, submitted to Rev. Sci. Instrum.
[38] C. Gil *et al.*, Fusion Science and Technology **56**, 1219 (2009)
[39] P. Hennequin *et al.*, Nuc. Fusion **46**, S771 (2006)
[40] M. Hirsch M. *et al.*, Plasma Phys. Control. Fusion **43**, 1641 (2001)
[41] T. N. Carlstrom *et al.*, Plasma Phys. Control. Fusion **44**, (2002)
[42] G. D. Conway *et al*., Plasma Phys. Control. Fusion **46**, 951 (2004)
[43] C. Fenzi *et al.*, Phys. Plasmas **12**, 062307 (2005)
[44] J. Schirmer *et al.*, Nuc. Fusion **46**, S780 (2006)
[45] C. Bourdelle *et al.*, Nuc. Fusion **42**, 892 (2002)
[46] A. M. Garofalo *et al.*, Phys. Rev. Letters **101**, 195005 (2008)
[47] W. Houlberg *et al*., Phys. Plasmas **4**, 3230 (1997)
[48] P. H. Diamond *et al.* Nuclear Fusion **49**, 045002 (2009)
[49] R. R. Dominguez *et al.*, Phys. Fluids B **5**, 3876 (1993)
[50] P. H. Diamond *et al.*, in Proc. of the 15th Int. Conf. on Plasma Phys. and Control. Nucl. Fusion, Seville, 1994 (IAEA, Vienna, 1995) Vol. 3, p. 323
[51] X. Garbet *et al.*, Phys. Plasmas **9**, 3893 (2002)
[52] P. H. Diamond *et al.*, Phys Plasmas **15**, 012303 (2008)
[53] Ö. D. Gürcan *et al.*, submitted to Phys. Plasmas (2010)
[54] L. Vermare *et al.*, Nuclear Fusion 46 (2006) S743-S759 (2006)
[55] T. S. Hahm *et al.*, Phys. Plasmas **14**, 072302 (2007)
[56] A. G. Peeters *et al.*, Phys. Rev. Lett. **98**, 265003 (2007)
[57] Ö. D. Gürcan *et al.*,Phys. Rev. Lett. **100**, 135001 (2008)
[58] C. Bourdelle *et al.*, Phys. Plasmas **14**, 112501 (2007)